

## Supporting Information

### **A $\text{Li}^+/\text{Zn}^{2+}$ Hybrid Electrolyte Revolutionizes V-MOF Cathode Performance and Zinc Anode Reversibility**

Yin Ma, <sup>a</sup> Yu Hu, <sup>a</sup> Yutong Meng, <sup>a</sup> Haihong Zhao, <sup>a</sup> Jiang Yin, <sup>a</sup> Xiangping Chen, <sup>a</sup>  
Liqiu Mao, <sup>\*a</sup> Xiongwei Wu, <sup>\*a</sup> Lishan Yang, <sup>\*a</sup>

<sup>1</sup> Key Laboratory of Chemical Biology & Traditional Chinese Medicine Research (Ministry of Education of China), National and Local Joint Engineering Laboratory for New Petrochemical Materials and Fine Utilization of Resources, Key Laboratory of the Assembly and Application of Organic Functional Molecules of Hunan Province, Hunan Normal University, Changsha, Hunan 410081, P.R. China

**\* Correspondence:**

mlq1010@126.com (L.Q.M.)

wxw@hunau.edu.cn (X.W.W.)

lsyang@hunnu.edu.cn (L.S.Y.)

Tel./Fax.: +86 731 88872531

---

## EXPERIMENTAL SECTION

### Materials synthesis

In this work, all chemicals were reagent grade and used as received from commercial sources without further purification. V(IV)(O)(bdc) powder was prepared using the solvothermal method. Briefly, 2.0 mmol (0.43 g) of  $\text{VOSO}_4 \cdot n\text{H}_2\text{O}$  and 4.0 mmol (0.64 g) of 1,4-benzenedicarboxylic acid were fully stirred in 40 mL of dimethylformamide (DMF) solution and ultrasonically treated for 1h, then transferred to a polytetrafluoroethylene lined stainless steel autoclave. The autoclave was maintained at 160 °C for 72 h, and then naturally cooled down to room temperature<sup>1,2</sup>. The yellow green powder was precipitated from the solution, filtered, fully washed with methanol, and then dried under vacuum at 80 °C for 24 h. Finally, the original V-MOF powder was annealed at 280 °C for 3 h in air to obtain hierarchical-porous V-MOF.

### Preparation of electrolyte solution

Preparation of pure  $\text{ZnSO}_4$  or  $\text{Li}_2\text{SO}_4$  electrolyte: Precisely weigh 0.075 mol of  $\text{ZnSO}_4 \cdot 7\text{H}_2\text{O}$  or  $\text{Li}_2\text{SO}_4 \cdot \text{H}_2\text{O}$ , dissolve in 15 mL of deionized water. After homogenization via ultrasonic agitation, transfer the solution to a 25 mL volumetric flask and dilute to the mark, resulting in a 3 M pure  $\text{ZnSO}_4$  or 3 M pure  $\text{Li}_2\text{SO}_4$  electrolyte solution.

Preparation of 3 M  $\text{ZnSO}_4$ +1 M  $\text{Li}_2\text{SO}_4$  hybrid electrolyte: Precisely weigh 0.025 mol of  $\text{Li}_2\text{SO}_4 \cdot \text{H}_2\text{O}$  and 0.075 mol  $\text{ZnSO}_4 \cdot 7\text{H}_2\text{O}$ , dissolve in 15 mL of deionized water, and homogenize via ultrasonication. Subsequently, transfer the solution to a 25 mL volumetric flask and bring to volume to obtain the 3 M  $\text{ZnSO}_4$ +1 M  $\text{Li}_2\text{SO}_4$  hybrid electrolyte.

### Materials characterization

The morphology of as-prepared samples was captured by a ZEISS Sigma 300 scanning electron microscope (SEM) at an acceleration voltage of 8.0 kV. The phase analysis of the samples was performed using a Bruker D8 Advance X-ray diffractometer (XRD) with  $\text{Cu K}\alpha$  radiation of 40 kV. The surface chemical species of the samples were examined using Thermo Scientific K-Alpha multifunctional X-ray photoelectron spectroscopy (XPS) with  $\text{Al K}\alpha$  radiation (1486.6 eV) as the excitation source. Transmission electron microscopy (TEM) images were obtained using a JEM-F200 microscope at an acceleration voltage of 200 kV. High-resolution TEM (HRTEM) images, selected area electron diffraction (SAED) images, and energy-dispersive spectrometer (EDS) mappings were captured using the same instrument. The surface areas and pore structure of the samples were measured by  $\text{N}_2$  adsorption/desorption experiments on a Micromeritics Accelerated Surface Area and Prosimetra System (ASAP2460). Fourier-transform infrared (FTIR) spectra were obtained using a Bruker Vertex 70v spectrometer. The Raman spectroscopy was obtained by a HORIBA Scientific LabRAM HR Evolution spectrometer.

### Electrochemical measurement

The electrochemical performances were evaluated using CR2032-type coin cells. Working electrodes were prepared by mixing the active materials, carbon black, and PVDF in a weight ratio of 70:15:15 in 1-Methyl-2-pyrrolidinone (NMP). The resulting slurry was scraped onto stainless steel mesh (100 mesh) and dried in vacuum at 80 °C for 12 h. The mass loading of the electrode material was  $\sim 1 \text{ mg cm}^{-2}$ . The CR2032-type

---

coin cell assembled in open air with a zinc plate served as the anode, glass fiber was used as the separator and 3 M ZnSO<sub>4</sub>+1 M Li<sub>2</sub>SO<sub>4</sub> was used as the aqueous electrolyte. Galvanostatic cycling tests of the assembled cells were conducted using a battery tester (Neware-BTS8 battery tester, China) in the voltage range of 0.2-1.6 V (vs. Zn<sup>2+</sup>/Zn) at various current densities.

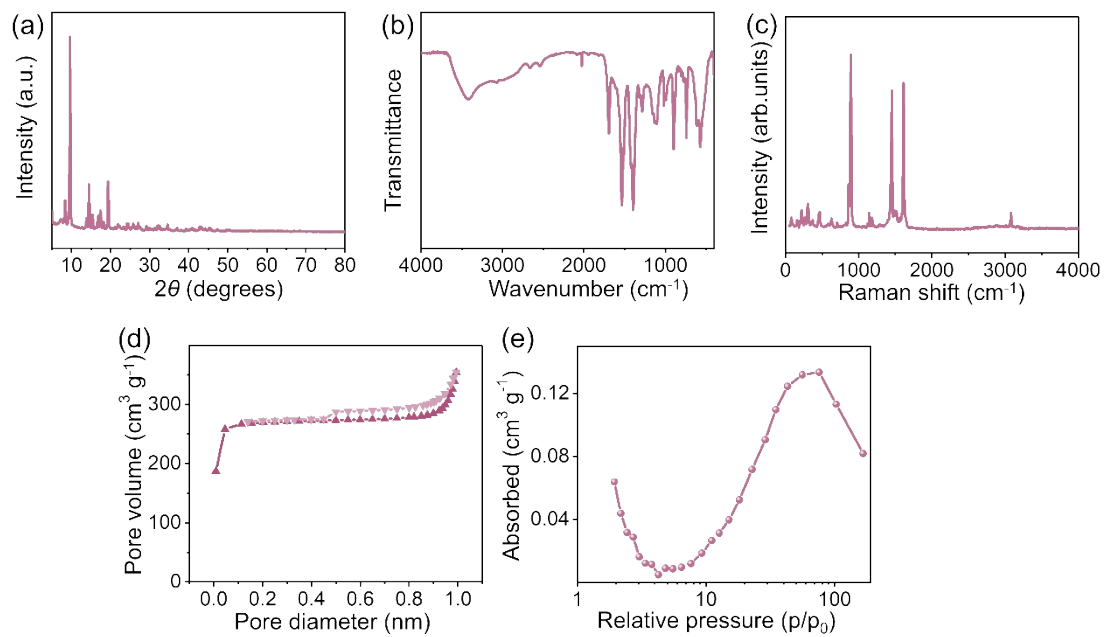


**Figure S1.** (a) XRD patterns, (b) FTIR patterns, (c) Raman shift, (d) Nitrogen adsorption/desorption isotherm, and (e) the corresponding pore-size distribution curves of V-MOF samples.

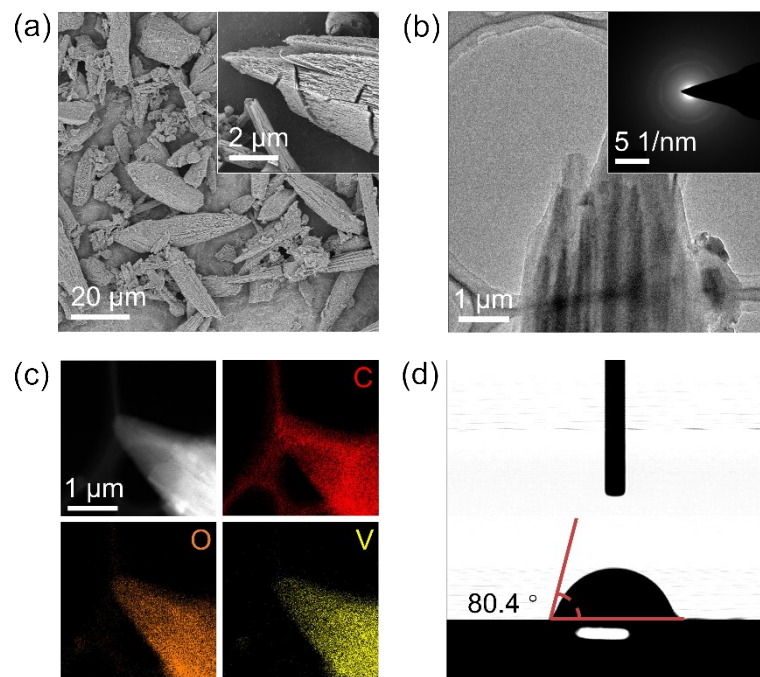


**Figure S2.** (a) SEM images, (b) TEM image and SAED pattern, (c) Dark-field STEM image and corresponding EDS elemental mappings of V-MOF sample. (d) Contact angle images for droplets water on V-MOF films.

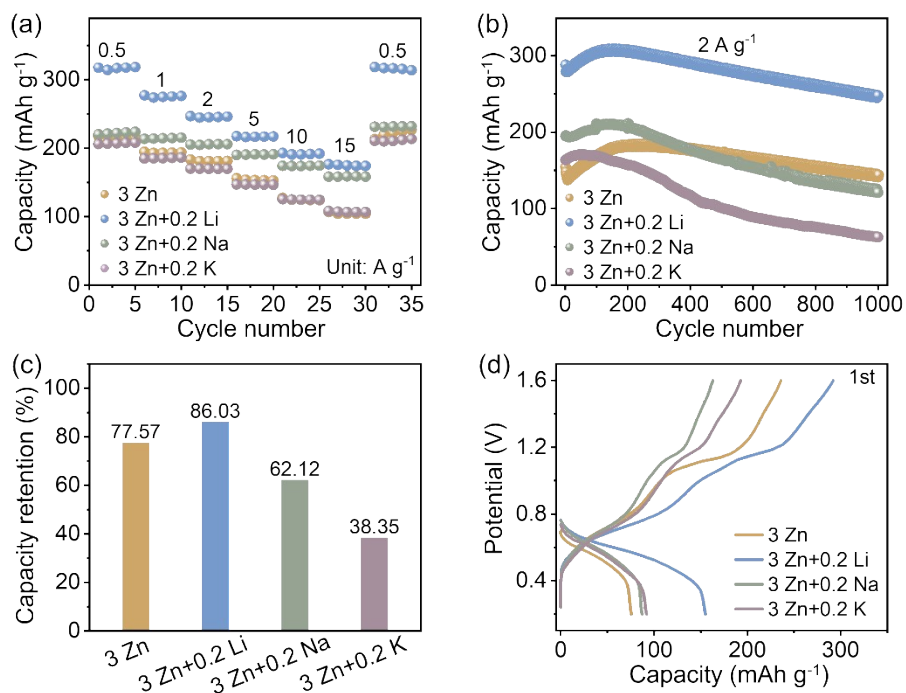


**Figure S3.** The comparison of Zn||V-MOF batteries in pure ZnSO<sub>4</sub>, Li<sup>+</sup>-ZnSO<sub>4</sub>, Na<sup>+</sup>-ZnSO<sub>4</sub> and K<sup>+</sup>-ZnSO<sub>4</sub> electrolytes: (a) Rate performance, (b) Cycling performance at 2 A g<sup>-1</sup>, (c) Capacity retention after 1000 cycles, (d) GCD curves.

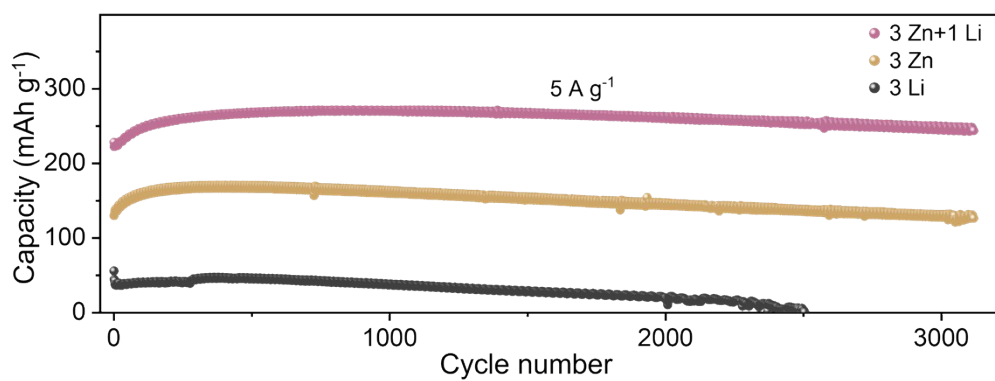


**Figure S4.** Cycling performance at 5 A g<sup>-1</sup> in Li<sub>2</sub>SO<sub>4</sub>, ZnSO<sub>4</sub> and Li<sup>+</sup>-ZnSO<sub>4</sub> electrolytes.

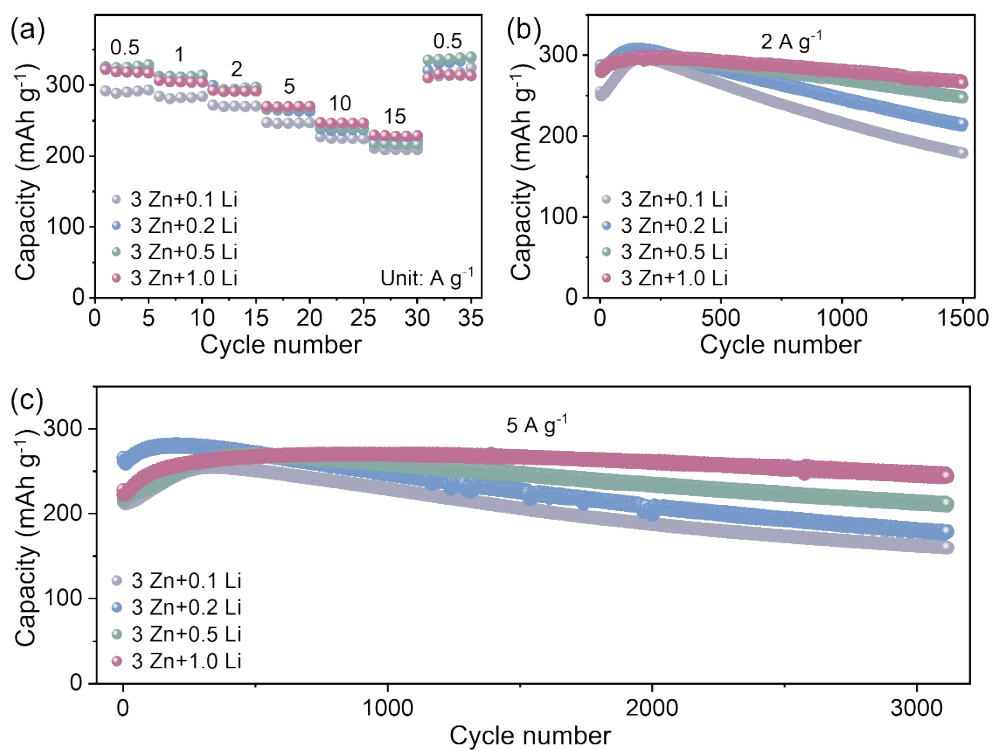


**Figure S5.** The comparison of Zn||V-MOF batteries in different concentration of Li<sup>+</sup> additives electrolyte (a) Rate performance, (b) Cycling performance at 2 A g<sup>-1</sup>, (c) Cycling performance at 5 A g<sup>-1</sup>.

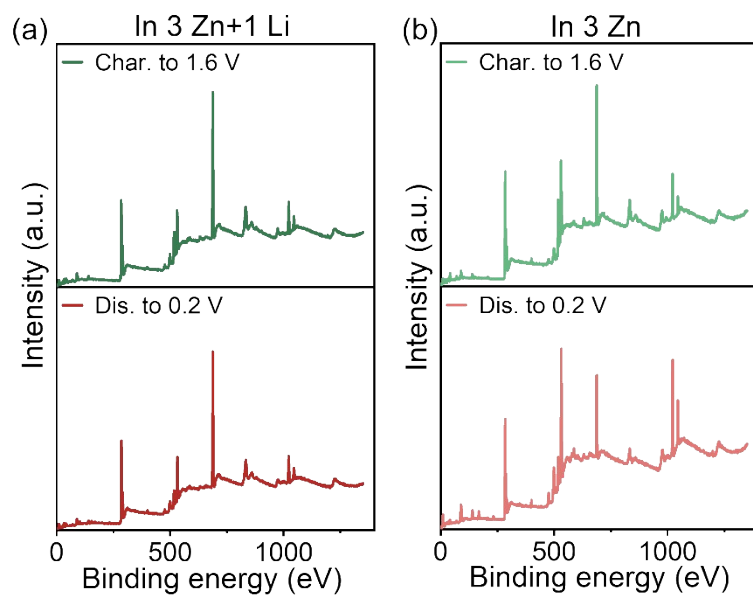


**Figure S6.** The survey XPS spectra of V-MOF in (a)  $\text{Li}^+$ - $\text{ZnSO}_4$  electrolyte, (b) pure  $\text{ZnSO}_4$  electrolyte.

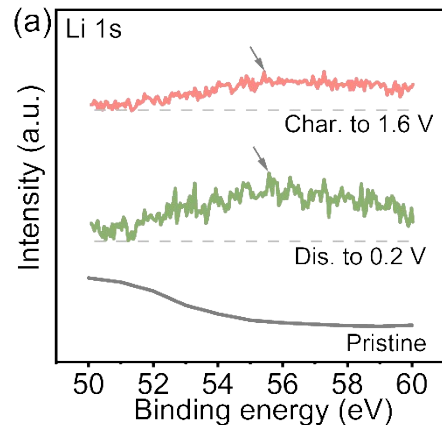


**Figure S7.** XPS curves of the Li 1s.

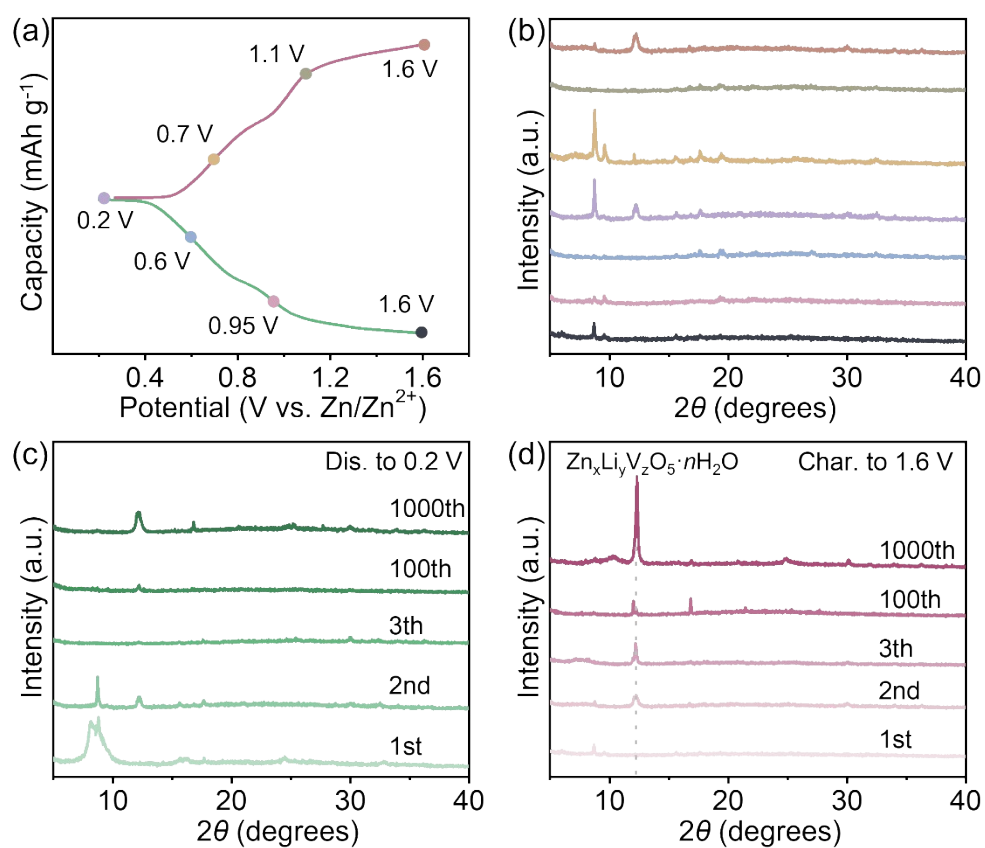


**Figure S8.** (a) The GCD curve for *ex-situ* analysis, (b) XRD patterns in different voltage at first cycle, (c) XRD patterns in different cycle numbers discharged to 0.2 V, (d) XRD patterns in different cycle numbers charged to 1.6 V of V-MOF cathode in  $\text{Li}^+$ - $\text{ZnSO}_4$  electrolytes.

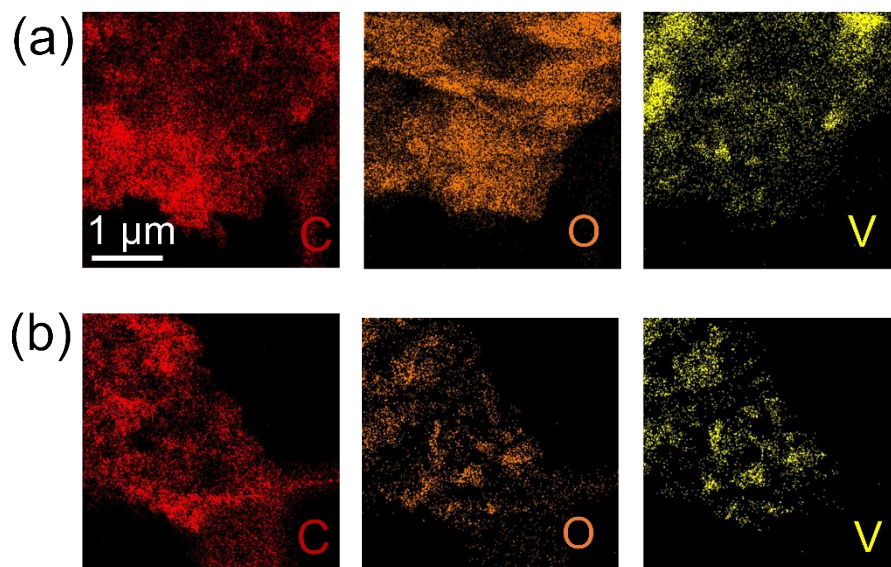


**Figure S9.** The corresponding EDS elemental mappings of the V-MOF electrode discharged to 0.2 V (a), and charged to 1.6 V (b) in  $\text{Li}^+$ - $\text{ZnSO}_4$  electrolyte.

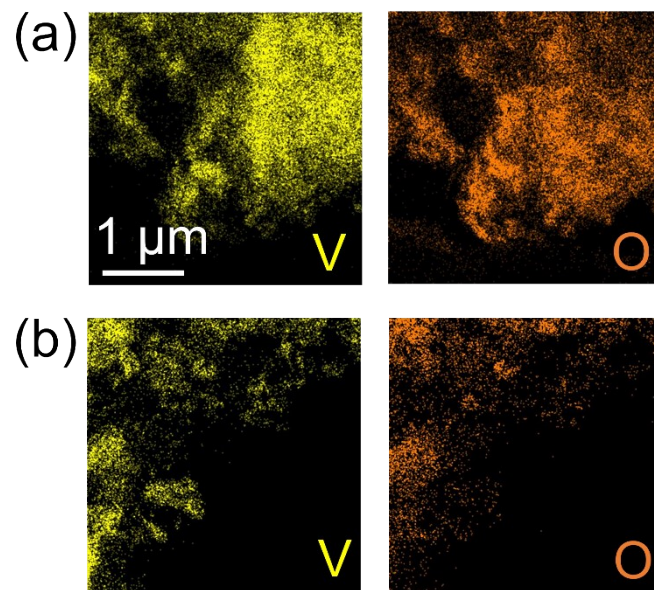


**Figure S10.** The corresponding EDS elemental mappings of the V-MOF electrode discharged to 0.2 V (a), and charged to 1.6 V (b) in ZnSO<sub>4</sub> electrolyte.

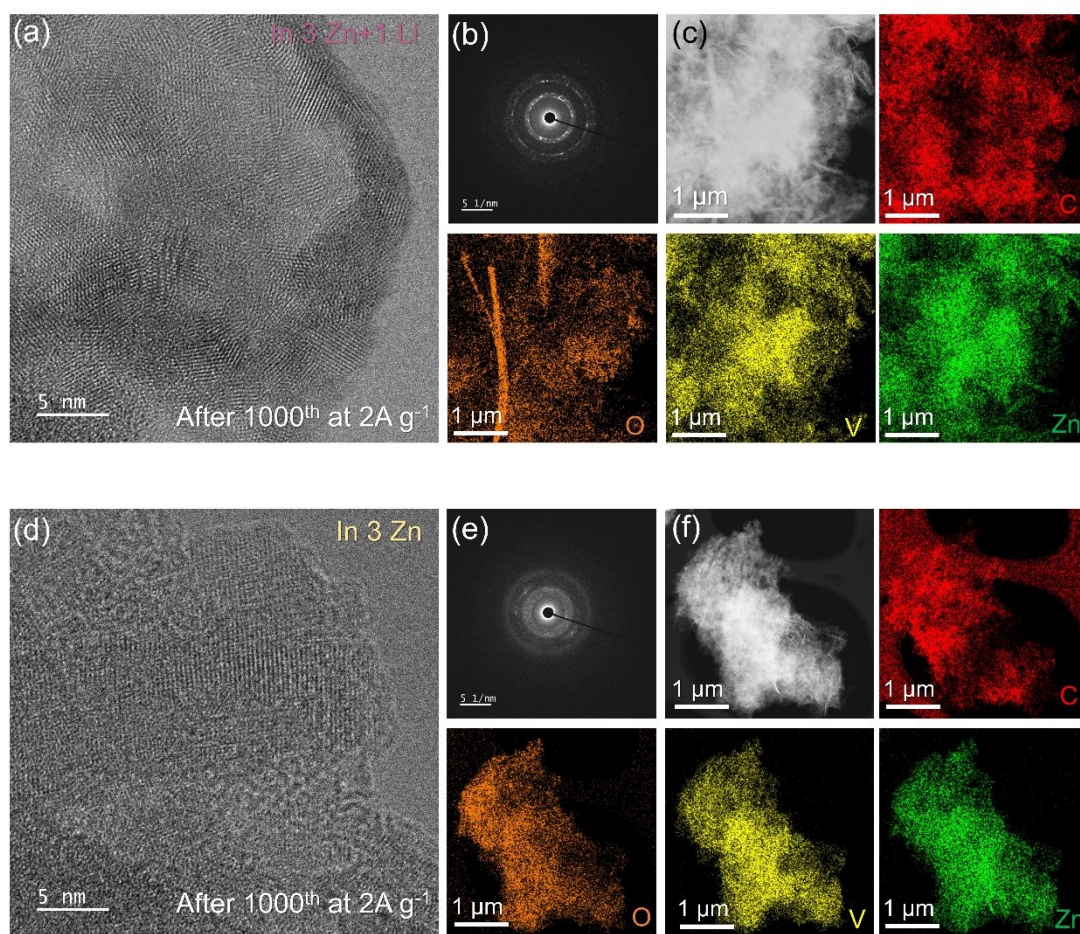


**Figure S11.** The HRTEM image, SAED patterns, bright-field STEM image, and corresponding EDS elemental mappings of the V-MOF in Li<sup>+</sup>-ZnSO<sub>4</sub> electrolyte (a-c) and ZnSO<sub>4</sub> electrolyte (d-f) after 1000 cycles at 2 A g<sup>-1</sup>.

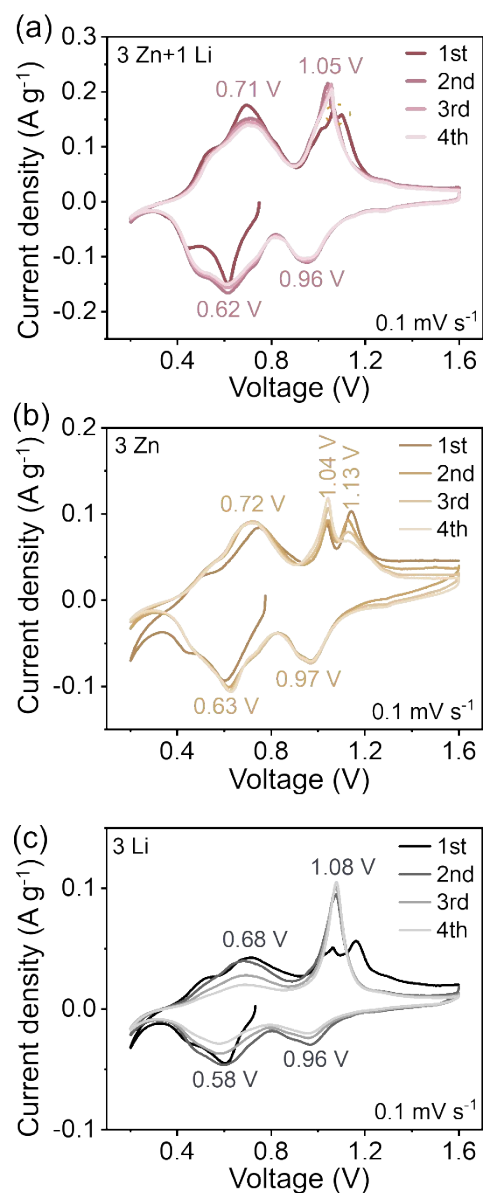


**Figure S12.** The CV curves of Zn||V-MOF batteries in (a) Li<sup>+</sup>-ZnSO<sub>4</sub> electrolyte, (b) pure ZnSO<sub>4</sub> electrolyte, (c) pure Li<sub>2</sub>SO<sub>4</sub> electrolyte.

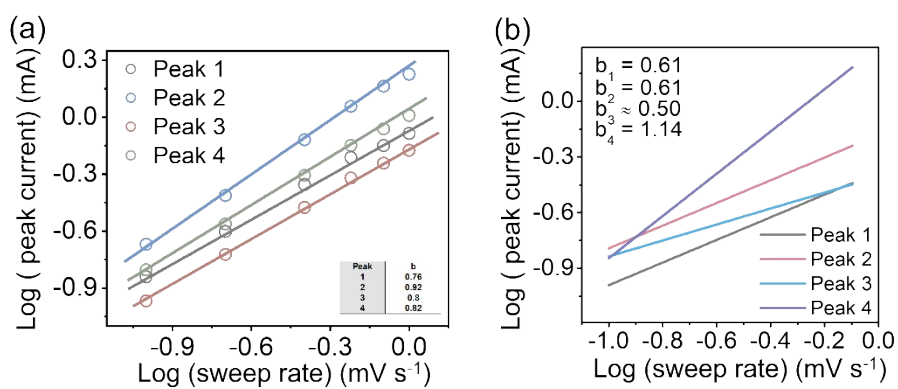


**Figure S13.** The corresponding  $b$ -values of the Zn||V-MOF batteries in (a) Li<sup>+</sup>-ZnSO<sub>4</sub> electrolyte and (b) ZnSO<sub>4</sub> electrolyte.

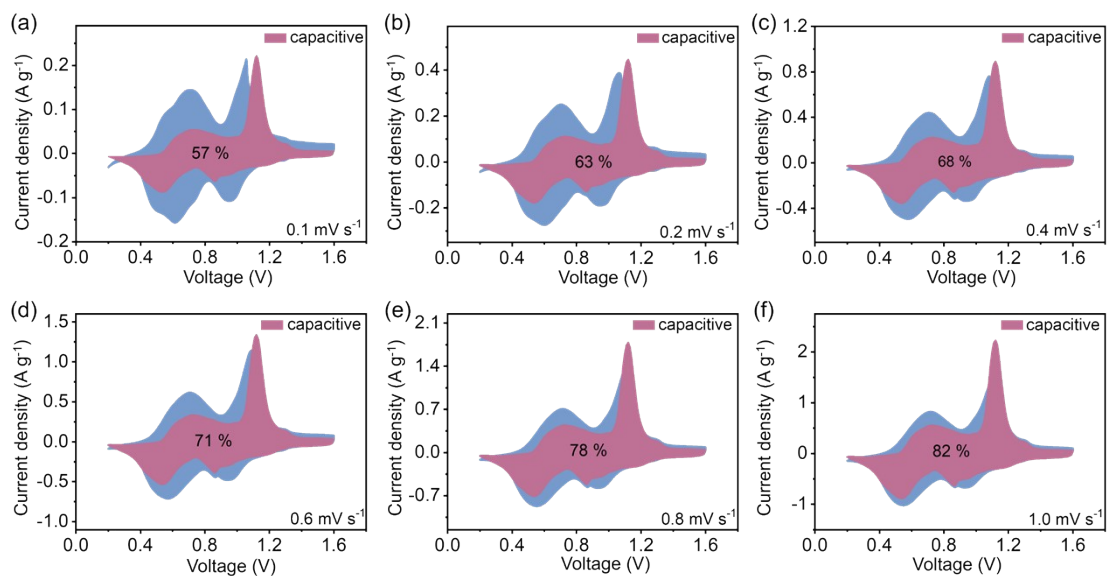


**Figure S14.** The fitting CV curves at different scan rates in Li<sup>+</sup>-ZnSO<sub>4</sub> electrolyte.

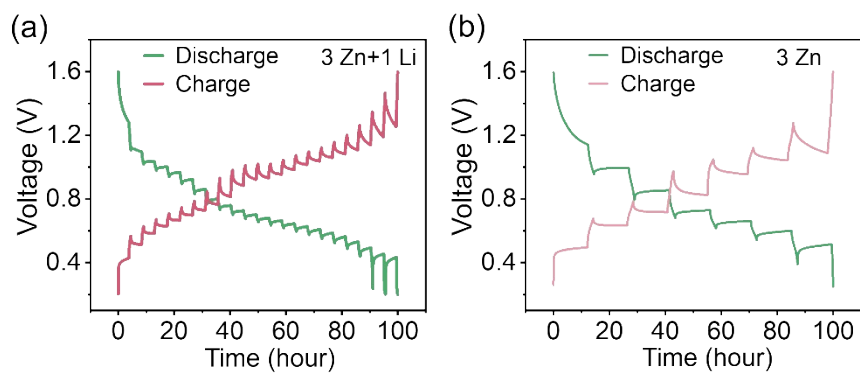


**Figure S15.** GITT curve of the Zn||V-MOF batteries in (a)  $\text{Li}^+$ - $\text{ZnSO}_4$  and (b)  $\text{ZnSO}_4$  electrolyte.



**Figure S16.** The electrical conductivity of (a) Li<sub>2</sub>SO<sub>4</sub>, (b) ZnSO<sub>4</sub> and (c) Li<sup>+</sup>-ZnSO<sub>4</sub> electrolyte (unit: 20m S cm<sup>-1</sup>).

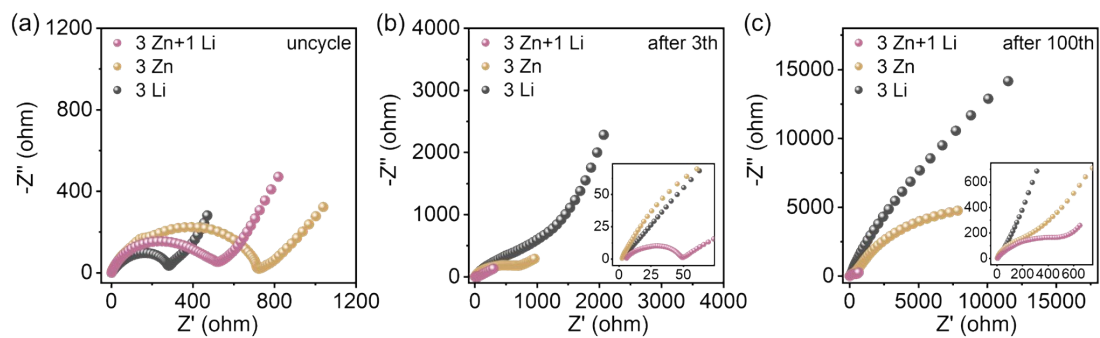


**Figure S17.** The comparison of Nyquist plots of (a) uncycled, (b) after 3 cycles and (c) after 1000 cycles in  $\text{Li}_2\text{SO}_4$ ,  $\text{ZnSO}_4$  and  $\text{Li}^+$ - $\text{ZnSO}_4$  electrolytes.

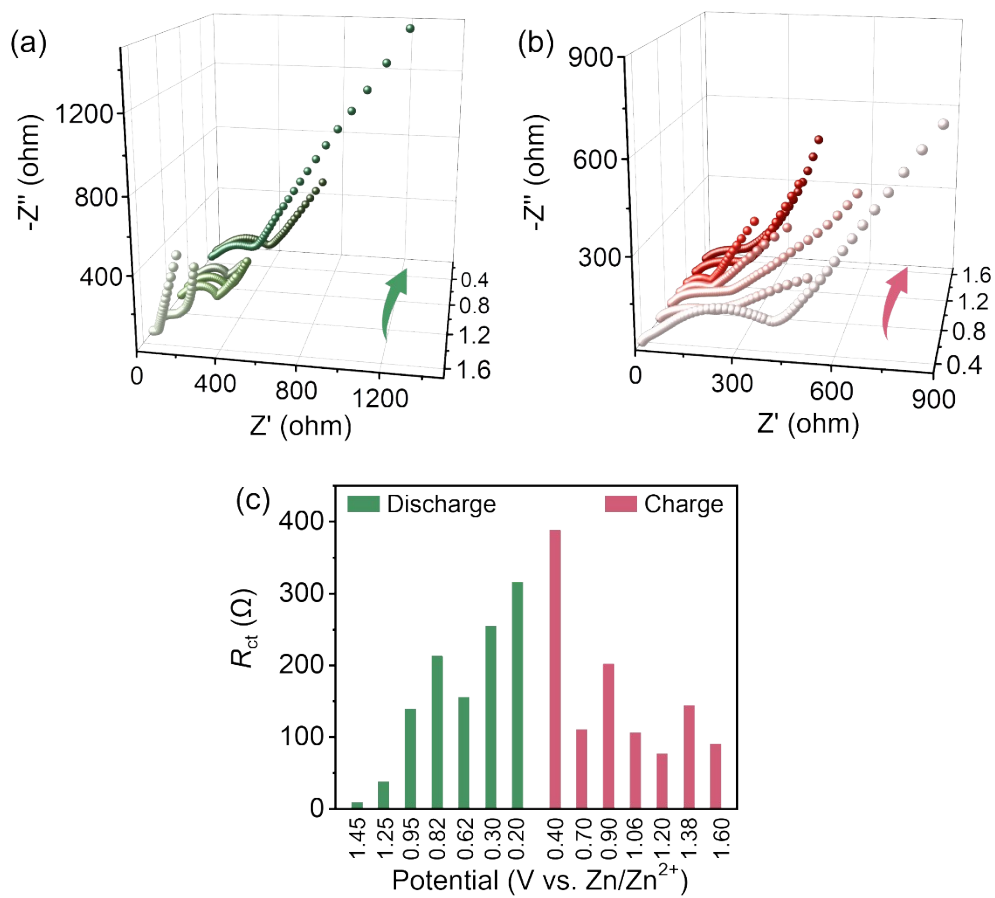


**Figure S18.** Ex-Nyquist plots at (a) discharging and (b) charging of Zn||V-MOF batteries in  $Li^+$ - $ZnSO_4$  electrolyte, (c) Corresponding equivalent resistance values.

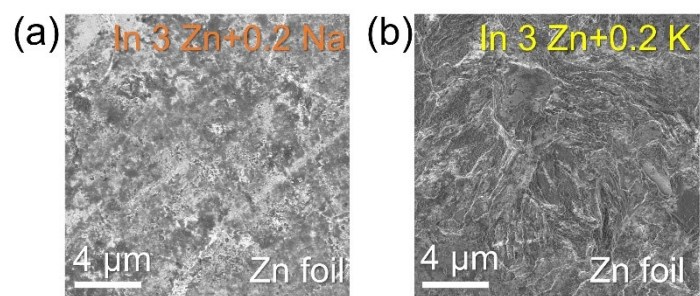


**Figure S19.** The SEM images of Zn electrode in (a) Na<sup>+</sup>-ZnSO<sub>4</sub> and (b) K<sup>+</sup>-ZnSO<sub>4</sub> electrolytes.

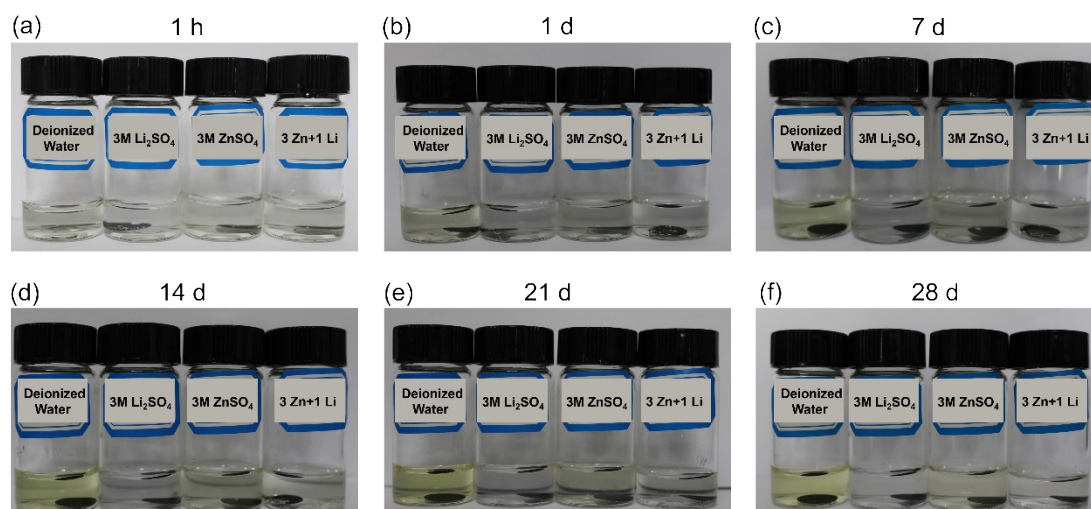


**Figure S20.** The images of V-MOF electrode in deionized water, 3 M Li<sub>2</sub>SO<sub>4</sub> electrolyte, 3 M ZnSO<sub>4</sub> electrolyte, and 1 M Li<sub>2</sub>SO<sub>4</sub> + 3 M ZnSO<sub>4</sub> electrolyte after different days.

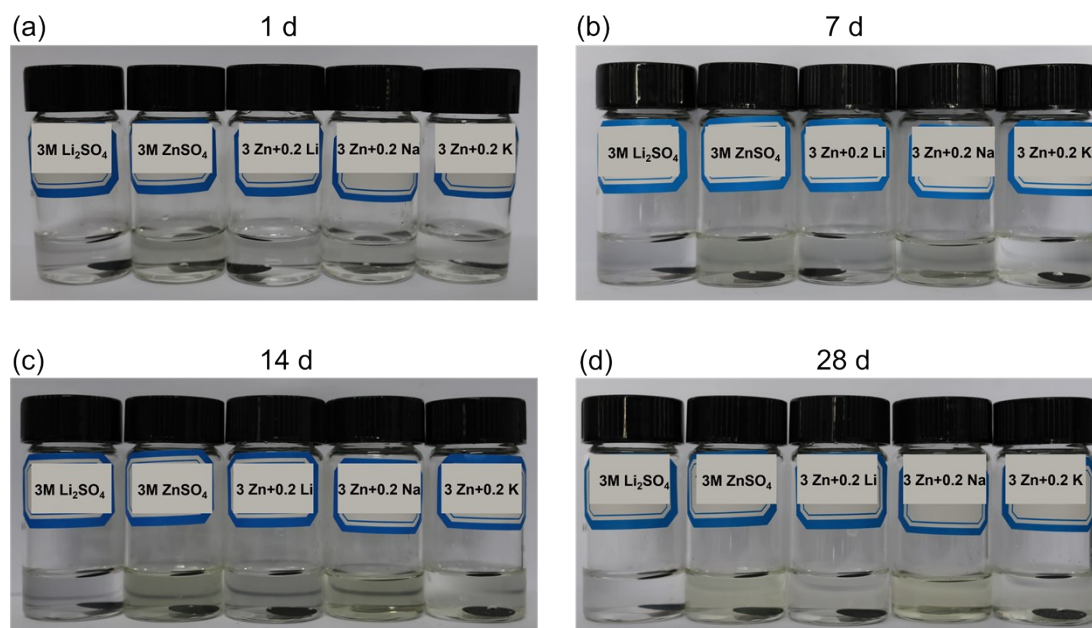


**Figure S21.** The images of V-MOF electrode in deionized water, 3 M Li<sub>2</sub>SO<sub>4</sub>, 3 M ZnSO<sub>4</sub>, 0.2 M Li<sub>2</sub>SO<sub>4</sub> + 3 M ZnSO<sub>4</sub>, 0.2 M Na<sub>2</sub>SO<sub>4</sub> + 3 M ZnSO<sub>4</sub>, and 0.2 M K<sub>2</sub>SO<sub>4</sub> + 3 M ZnSO<sub>4</sub> electrolyte after different days.

---

**Table 1** XPS results of V-MOF electrode in Li<sup>+</sup>-ZnSO<sub>4</sub> electrolyte (Atomic ratio /%)

3 Zn+1 Li	C	O	V	Zn	Li
Initial	65.93	28.03	6.01		
Dis. to 0.2 V	71.4		5.56	4.24	18.71
Char. to 1.6 V	63.51		9.08	4.81	22.61
2th Dis. to 0.2 V	52.16		7.62	11.96	28.27

---

---

**Table 2.** XPS results of the V-MOF electrode in ZnSO<sub>4</sub> electrolyte (Atomic ratio /%)

3 M ZnSO <sub>4</sub>	C	O	V	Zn	V/Zn
Initial	65.93	28.03	6.01	0	
Dis. to 0.2 V	61.75	29.11	2.26	6.89	1:3
Char. to 1.6 V	72.71	19.67	4.38	3.24	1:0.74

---

---

**Table S3.** Comparison for electrochemical performance of various cathode materials in ZIBs

Samples	Initial discharge capacity (mAh g <sup>-1</sup> )	Cycle number, discharge capacity (mAh g <sup>-1</sup> ) / capacity retention, discharge rate
This work	336.2 at 0.5 A g <sup>-1</sup>	3200th, 247.7/90.7 %, at 5 A g <sup>-1</sup>
V-MOF	183.3 at 0.05 A g <sup>-1</sup>	70th, 80/58.6 %, at 1 A g <sup>-1</sup>
Ni-MOF	139.4 at 2.5 A g <sup>-1</sup>	950th, 104.7/77.2 %, at 10 A g <sup>-1</sup>
Mn-MOF	170 at 0.05 A g <sup>-1</sup>	50th, 150, at 0.1 A g <sup>-1</sup>
Cu-MOF	228 at 0.05 A g <sup>-1</sup>	500th, 93.3/75 % at 4 A g <sup>-1</sup>

---

- 
1. Y. Yan, Y. Luo, J. Ma, B. Li, H. Xue and H. Pang, *Small*, 2018, **14**, 1801815.
  2. Y. Ma, D. Xiong, Y. Meng, Y. Lu, P. Duan, B. Chen, Y. Yang, X. Chen, L. Mao, X. Wu and L. Yang, *Sci. China Mater.*, 2025, **68**, 2764-2774.